SAND2016-11089C

Experimental Execution of 6DOF Tests Derived from Field Tests

Laura D. Jacobs[1], Senior Member of Technical Staff
Michael Ross, Principal Member of Technical Staff
Gregory Tipton, Distinguished Member of Technical Staff
Kevin Cross, Senior Member of Technical Staff
Norman Hunter Jr., Contract Associate
Julie Harvie, Member of Technical Staff
Garrett Nelson, Post-Doctoral Appointee
Vibration/Acoustics Simulation, Sandia National Laboratories[2]
P.O. Box 5800 MS 0557, Albuquerque, NM 87185

Abstract

Recent advances in 6DOF testing has made 6DOF subsystem/component testing a preferred method because field environments are inherently multidimensional and can be better replicated with this technology. Unfortunately, it is rare that there is sufficient instrumentation in a field test to derive 6DOF inputs. One of the most challenging aspects of the test inputs to derive is the cross spectra. Unfortunately, if cross spectra are poorly defined, it makes executing the tests on a shaker difficult. In this study, tests were carried out using the inputs derived by four different inverse methods, as described in a companion paper. The tests were run with all 6DOF as well with just the three translational degrees of freedom. To evaluate the best way to handle the cross spectra, three different sets of tests were run: with no cross terms defined, with only the coherence defined, and with the coherence and phase defined. All of the different tests were compared using a variety of metrics to assess the efficacy of the specification methods. The drive requirements for the different methods are also compared to evaluate how the specifications affect the shaker performance. A number of the inverse methods show great promise for being able to derive inputs to a 6DOF shaker to replicate the flight environments.

Keywords

Multi-axis, Vibration, Experimental, Structural Response, Dynamics

Introduction

The vast majority of product life-cycle and environmental vibration tests are currently conducted on uniaxial vibration test platforms. These tests have been established as a method to detect part failures and predict the effects of service loads without the need of costly and time consuming field testing. The most widely referenced standard for these tests, MIL-STD-810G, specifies the use of sequential single axis tests in each of three orthogonal axes to characterize and validate the performance of both components and assemblies [2]. Comparable methods are provided by the U.S. Navy in NAVMAT P-9492 and the electronics industry's JESD22-B103B [3, 4]. Per the guidance given by these standards, the device is first tested along a single axis and then rotated 90° about the appropriate axis, with a test conducted after each rotation.

In the past few decades, advances in multi-axis testing hardware and software solutions have increased the application of multi-axis testing at both the system and component level. Vibration systems capable of multi-axis simulation have been successfully incorporated in both research and development labs across the U.S. in universities, government labs, and industry alike [5, 6, 7, 8, 9, 10]. Their increased prevalence is motivated by a growing body of evidence which indicates shortcomings in conventional single axis testing [11]. In many environments, the effects of cross-axis excitation can have

---

[1] ldjacob@sandia.gov
[2] Sandia is a multi-program laboratory operated by Sandia Corporation, a Lockheed Martin Company, for the United States Department of Energy under contract DE-AC04-94AL85000.

large impacts on the resulting dynamics of a structure [12]. Accordingly, it has been found that the combined loading effects caused by these multi-axis excitations can result in different stress states [13, 14, 15], failure modes [16], and rates of damage accumulation [17, 18, 19]. Thus, it is no surprise that multi-axis testing has been shown to produce loading conditions that more closely simulate real world environments [20, 21]. This has motivated a dramatic increase in research on multi-axis test methods and the tools and analysis techniques necessary to make this testing possible. One key research area, and the focus of the present discussion, is the development of specifications for multi-axis testing.

In general, multi-axis vibration test specifications require the definition of a desired energy level and distribution for each axis as well as a definition for the relationship between each pair of axes. For random vibration tests, the specification for each independent axis is most commonly defined by an auto spectral density (ASD). As a function of frequency, the ASD specifies the level of energy in units of g^2/Hz. For a multi-axis specification, the relationship between each axis can be defined by the cross power spectral density (CPSD). For convenience and increased physical understanding, this relationship is often presented as a frequency dependent coherence and phase. Collectively, the ASDs and CPSDs fully define the desired input conditions for the test.

Traditional multi-axis testing is conducted by developing a control scheme based on rigid body acceleration at the base of a component, assembly, or fixture [22]. Unfortunately, due to limits on the number of channels available for data acquisition during field tests, it is rare to have sufficient instrumentation such that six degree of freedom (6-DOF) inputs can be directly derived at either the system or sub-system level. Specifically, the coherence and phase between axes is not adequately quantified and little to no data is available for rotational acceleration measurements. This has led to the development of various methods to derive test specifications and inputs by pairing field data with analysis on a dynamic model of the system of interest. Depending on the availability of a high fidelity finite element model of the unit under investigation, alternate experimental model techniques may be employed.

A recent field test conducted by Sandia National Laboratories on a system level assembly was instrumented specifically such that these multi-axis inputs could be directly measured. In addition to providing an input signal which could be used directly for multi-axis testing, this set of field data also provided the unique opportunity to benchmark the performance of other methods for deriving 6-DOF test inputs from field data with limited instrumentation. This was possible by comparing the results of tests conducted with input signals derived from only response channels which would have been available during a standard field test to those conducted with the "true" input signals which were directly measured. Specifically, four different multi-axis input specification derivation methods were explored: (1) using the pseudo-inverse of the transmissibility function (PINV), (2) the output spectral density method (ZINV), (3) a scaled output spectral density method (Scaling), and (4) an iterative spectral density method with Tikhonov regularization (Smallwood-Cap). These methods are discussed further in the companion paper [24]. In addition to comparing the estimate of input signal obtained from each method, the dynamic response of the test article to these derived inputs were experimentally obtained on a shaker system and compared to measurement response data from the original field test. Comparisons were made with a set of 7 measurement locations which were consistent between the lab and field tests. Objective measures of the performance of each method were based on both time and frequency domain characteristics of the data.

Test Setup

Instrumentation

The test article was equipped with an array of triaxial accelerometers for control. Additional accelerometers were placed in key locations internally to the system. The four control accelerometers were positioned symmetrically about both lateral axes at the mid-plane of the test article's base for testing on the multi-axis system. The locations of the control gauges and internal gauges are shown notionally in Fig. 1.

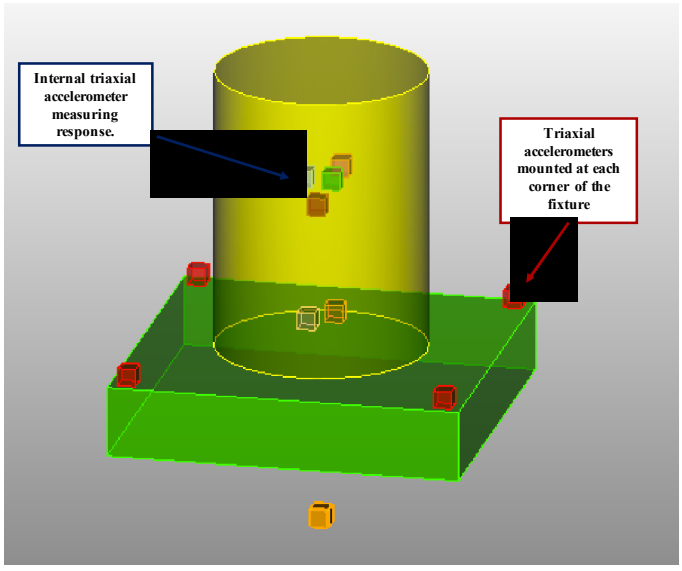

Fig. 1 Notional depiction of test article and accelerometers

Test Equipment

For physical testing conducted on the system, Team Corporation's Tensor 18kN (TE6-18kN) multi-axis high frequency vibration test system was employed (see Fig. 2). Due to the test equipment's configuration of twelve independent electrodynamic shakers, by controlling the relative amplitude and phase of the various shakers, it is capable of full six degree of freedom (6DOF) vibration testing.

Fig. 2 Tensor 18kN multi-axis vibration test system [23]

Test Specifications

Several different tests were specified. In addition to conducting tests that were specified using the different input derivation methods described in the companion paper [24], different methods for determining the cross spectra were also explored: no cross spectra, coherence only, and coherence with phase. Additionally, the tests were performed using the three translational degrees of freedom (3DOF tests) only and the three translational degrees of freedom with the addition of the three rotational degrees of freedom (6DOF tests).

Experimental Results

Visual Comparison

Doing a visual inspection of the response of the system to the various inputs provides some valuable insight into some general trends of the behavior of the system in the lab versus what was seen in the field. The visual inspection shows some clear differences between the 3DOF testing (Fig. 3 (a)) and the 6DoF testing (Fig. 3 (b)).

One general trend of the 3DOF testing (Fig. 3 (a)) is that, with the exception of the Smallwood-Cap input, the 3DOF inputs led to responses on the test article that contained significantly less energy from 20 to 200Hz and 300 to 600Hz. At higher frequencies, with exception of a few shifts in the peaks and valleys, the responses of each 3DOF test were reasonably similar to those in field testing. The low frequency peaks line up well, even though they are a lower amplitude. In other words, the shapes of the PSDs at lower frequencies are similar. The PSDs at higher frequencies differ from those measured in the field test. This result is unsurprising because the unit to unit variability in the dynamics were more pronounced at the higher frequencies. Many of the modes appear to have less damping than they did during field testing, because they have higher amplitudes and sharper peaks than the ones in field testing. It is possible that the change in boundary condition affects the apparent damping of the system.

One of the interesting trends in the 6DOF data ((Fig. 3 (b)) is that the responses are higher across the entire frequency range. This result suggests that adding the rotations makes certain modes more pronounced. It was also easier to recreate one of the rigid body modes that is transferred into the system when rotations were included. Although the shapes of the PSDs demonstrate close agreement at frequencies below 1000Hz, the peaks are somewhat shifted and are a higher amplitude than those found in the field test. Above 1000Hz, the response of the system in the laboratory test was significantly higher than the response in the field test. The rotations appear to have a significant effect on the higher frequencies.

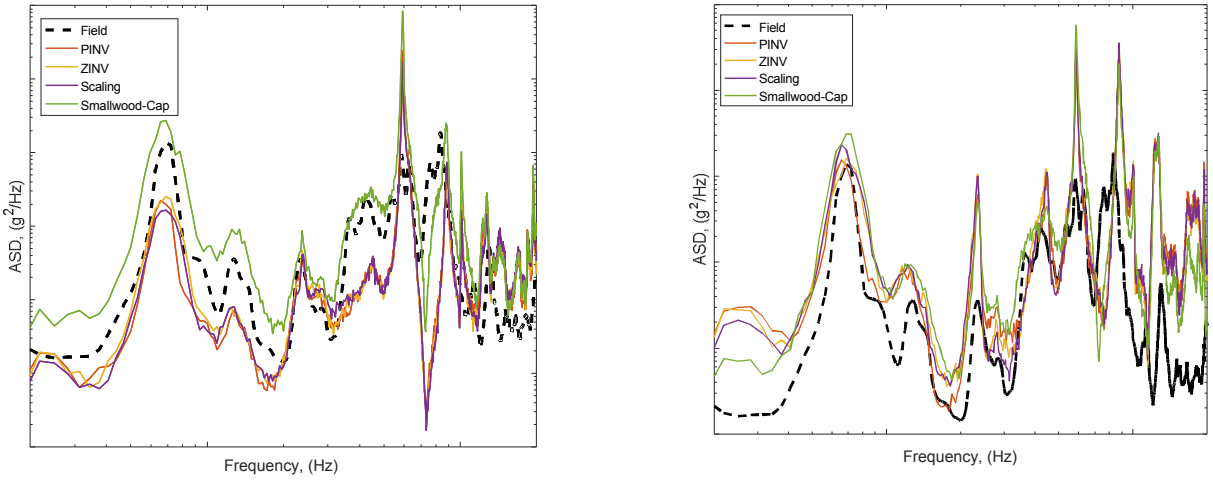

(a) (b)

Fig. 3 Response of the System to (a) 3DOF Inputs (b) 6DOF Inputs

Although a visual inspection of the various responses can be used to gain valuable insight about the different methods employed, it is challenging to determine which of the methods of defining the specifications leads to the closest match to what was seen in the field test. Therefore, quantitative metrics should be used to make a clear determination of the best method.

Methods for Comparison

One of the goals of this study is to evaluate how well each of the methods of defining the inputs did at replicating the response measured during the field test and determine which one is most promising. In order to do that, a variety of metrics were calculated and compared to one another. The metrics were combined using equal weighting.

A few different features are of interest when comparing the laboratory response to that measured in the field test. The first feature is the shape of the PSD curve, which gives information about the frequency content of the response. One of the things to consider in comparing the shape, is that small differences in the natural frequencies between the field test and laboratory units could show up in the PSD, so having some leeway in the exact locations of the peaks in the PSD would be valuable in a metric, so small shifts are not heavily penalized. The second feature is the overall energy in the response.

The first step in calculating the metrics is to convert the data to sixth octave spacing. This means that there are six frequency lines per octave, with their corresponding amplitudes of the PSD. Since octaves represent a doubling of frequency, more frequency lines are averaged at the higher frequencies than the lower frequencies. This technique helps to remove some of the jitter seen at the higher frequencies as well as smooth out some of the slight shifts in frequency due to unit to unit variability.

The first metric is the error in the rms, which is a way to compare the energy levels from the laboratory test and the field test. The rms for both the field test and laboratory data were calculated by finding the area under the PSD curve. Calculating the error for each gauge can be done by using the following equation:

$$error_{rms} = 20\log\left(\frac{rms_{test}}{rms_{flight}}\right) \quad (1)$$

Summing the error of each gauge gives the total error in the rms across the system.

In order to be able to weight each metric equally, the error in the rms needed to be converted to a number between 0 and 1, where 1 is the value associated with the smallest error in the rms. This was accomplished by first using the following equation:

$$\boldsymbol{normalized_{rms} = 1 - \frac{TotalRmsError}{MaxRmsError}} \quad (2)$$

which gives a set of metrics where now the largest one is associated with the test that had the smallest error in the rms. Then, to make the one with the smallest error have a value of 1, the following equation is applied

$$\boldsymbol{metric_{rms} = \frac{normalized_{rms}}{\max(normalized_{rms})}} \quad (3)$$

The next metric is the mean dB error, which is another way to compare the energy between the laboratory test and the field test. This metric calculates the dB error at each frequency line and then performs an average over all frequencies. This metric can be sensitive to small shifts in the natural frequencies inherent to unit to unit variability. The mean dB error is calculated as follows:

$$\boldsymbol{error_{dB} = \frac{1}{N}\sum_{f_{min}}^{f_{max}} 10\left(\log\left(\frac{test(f)}{flight(f)}\right)\right)} \quad (4)$$

The mean dB error can then be summed across all the gauges to get a single metric for each test method. The normalization is calculated in the same manner as the error in the rms, using the following equation

$$\boldsymbol{normalized_{dB} = 1 - \frac{TotaldBError}{MaxdBError}} \quad (5)$$

which gives a set of metrics where now the largest one is associated with the test that had the smallest error in the rms. Then, to make the one with the smallest error have a metric of 1, the following equation is applied

$$\boldsymbol{metric_{dB} = \frac{normalized_{dB}}{\max(normalized_{dB})}} \quad \textbf{(6)}$$

The next metric is the correlation coefficient, which is a way to compare the shapes of the PSDs. This gives an indication of how well the two PSDs match in terms of amplitudes at each frequency line. One disadvantage to this metric is that small shifts in the natural frequencies can be heavily penalized because peaks can line up with valleys in more than one place. The correlation coefficient is calculated using the corrcoef function in Matlab to compare the PSDs of each location during the test to the PSD of the same locations in the field test. The correlation coefficient is a number between -1 and 1, where 1 is perfect correlation, 0 is completely uncorrelated, and -1 is perfectly negatively correlated. To get a number between 0 and 1, the following equation is used:

$$\boldsymbol{normalized_{corr} = 10(corr + 1)} \quad (7)$$

Then, to make the one with the smallest error have a value of 1, the following equation is applied

$$\boldsymbol{metric_{corr} = \frac{normalized_{corr}}{\max(normalized_{corr})}} \quad (8)$$

One way to get around the problem of small shifts in the natural frequencies is to calculate the cross correlation. Like the correlation it can give an indication the two PSDs match, but the cross correlation is a measure of similarity when there is a lag present, which means that it is more forgiving of small shifts in the natural frequencies. The cross-correlation coefficient is calculated using the xcorr function in Matlab to compare the PSDs of each location during the test to the PSD of the same locations in the field test. The cross-correlation coefficient is a number between -1 and 1, where 1 is perfect correlation, 0 is completely uncorrelated, and -1 is perfectly negatively correlated. To get a number between 0 and 1, the following equation is used:

$$\boldsymbol{normalized_{xcorr} = 10(xcorr + 1)} \quad (9)$$

Then, to make the one with the smallest error have a value of 1, the following equation is applied

$$\boldsymbol{metric_{xcorr} = \frac{normalized_{xcorr}}{\max(normalized_{xcorr})}} \quad (10)$$

Results

In addition to the different methods for deriving the inputs that were described in the companion paper [24], different methods for determining the cross spectra were used: no cross spectra, coherence only, and coherence with phase. Additionally, the tests were performed using the three translational degrees of freedom (3DOF tests) as well as the three translational degrees of freedom with the three rotational degrees of freedom (6DOF tests). Table 1 summarizes the results of the comparison between the different methods of deriving specifications for this set of tests.

Table 1. Comparison Metrics between Laboratory Tests and Field Tests

Method	No Cross Products		Coherence Only		Coherence & Phase	
	Metric	Rank	Metric	Rank	Metric	Rank
6th Octave 3DoF	2.710	14	++	++	++	++
6th Octave 6DoF	1.935	25	++	++	++	++
PINV 3DoF	3.139	8	2.938	12	3.253	5
PINV 6DoF	2.707	15	2.457	17	2.187	23
ZINV 3DoF	3.140	7	2.934	13	3.324	4
ZINV 6DoF	2.411	19	2.278	21	2.444	18
Scaling 3DoF	3.032	9	2.681	16	3.025	10
Scaling 6DoF	2.220	22	2.323	20	2.034	24
Smallwood-Cap 3DOF	3.152	6	3.723	2	3.763	1
Smallwood-Cap 6DOF	**	**	3.005	11	3.372	3

** No data available

++ Not Specified

The response of the system in the lab did not exactly match the response of the system in the field. In fact, using the full 6DOF inputs measured in the field yielded responses that were least like those in the field. This result can be understood in lieu of the fact that the boundary conditions in the field and the laboratory are different. In general, a change in boundary conditions will lead to differing dynamic responses. Additionally, the unit tested in the laboratory was different than the one used in the field test, and the unit to unit variability is going to lead to differences in the dynamic response. However, using an inverse method that accounts for the response of the structure on the shaker allowed for the laboratory response to be closer to that measured in the field test.

Another interesting trend is that, across the board, the metrics indicate that 3DOF tests matched the field data better than their 6DOF counterparts that were derived using the same methods. One possible explanation for this difference is that the rotations are more susceptible to both the variations in the parts and the change in boundary conditions than are the translations.

The Smallwood-Cap 3DOF method gave the best match to the field test data, no matter how the cross spectra were defined. Including the coherence and phase in the Smallwood-Cap method yielded the responses that matched the most closely to those measured in the field. In fact, for 5 out of the 8 inverse methods, including the coherence and phase yielded the closest match with the field data. This is unsurprising as the dynamic response of the system is coupled between axes. Additionally, the vibration input into the system in the field test has coupling between axes, so including that in the specifications in the laboratory would be expected to yield responses that are closer to those in the field test. Of the remaining three, two of the methods yielded the closest match to the field test when both coherence and phase were not specified.

From the initial look at the data for the tests run to 2kHz, the laboratory inputs should be derived using an inverse method, they should be 3DOF inputs, and the spectral density matrix should include both the coherence and phase. It is also recommended that the Smallwood-Cap method be used.

CONCLUSIONS

Recent field tests at Sandia National Laboratories had sufficient instrumentation to derive the full 6DOF base inputs to a system using a variety of methods. Testing in the laboratory implemented the different inputs and the response at 7 key locations were measured. The responses at the 7 key locations were compared to those measured in the field testing and a few key trends were apparent in the data.

With the exception of the Smallwood-Cap method, the 3DOF input produced a response that was lower than that of the field data. Conversely, the 6DOF input produced a response that matched well at low frequencies, but was too high at the higher frequencies.

Using an inverse method, rather than the inputs directly calculated from the field data seemed to yield internal responses that were closer to those measured in the field. Performing an inverse calculation based on transfer functions of the system on the shaker seems to remove some of the effects of the different boundary condition as well as the unit to unit variability.

It was very difficult to use a visual inspection of the data to draw any conclusions about which of the methods performed best. Therefore, it was necessary to use quantitative metrics to objectively assess how well the various input derivations performed. The metrics quantified how well the energy input as well as how well the shape of the PSDs matched between the field data and the laboratory simulations. Multiple metrics were necessary to capture both of these quantities.

In every instance, the metrics indicate that 3DOF tests matched the field data better than their 6DOF counterparts that were derived using the same methods. The Smallwood-Cap 3DOF method gave the best match to the field test data, no matter how the cross spectra were defined. However, including the coherence and phase in the Smallwood-Cap method yielded the responses that matched the most closely to those measured in the field. In general, including both the coherence and phase improved the response of the system.

Based on the results, it is recommended to use an inverse method to derive the inputs rather than relying on the measured field data. Also, the inputs should be 3DOF inputs rather than 6DOF inputs and the spectral density matrix should include the coherence and phase. Finally, it is recommended that the Smallwood-Cap method be used.

References

[1] J. M. Sater, C. R. Crowe, R. Antcliff and A. Das, "An assessment of smart air and space structures: demonstrations and technology," Institute for Defense Analyses, Alexandria, VA, 2000.

[2] U.S. Department of Defense, "Environmental engineering considerations and laboratory tests," 2008.

[3] U.S. Navy, "Manufacturing screening test standards," 1979.

[4] Joint Electron Device Engineering Council, "JEDEC standard: vibration variable frequency," 2006.

[5] C. Choi, M. Al-Bassyiouni, A. Dasgupta and M. Osterman, "PoF issues in multi-dof vibration testing: ED shakers and RS shakersq," in *IEEE Accelerated Stress Testing and Reliability Conf.*, New Jersey, 2009.

[6] M. J. Shafer, D. R. Wilson and R. V. Johnson, "New ICBM shock and vibration test capabilities at OOALC's Survivability and Vulnerability Integration Center," in *Proc. Joint Services Data Exchange Conf.*, 1994.

[7] M. Chen and D. Wilson, "The new triaxial shock and vibration test system at Hill Air Force Base," *J. IEST,* vol. 41, no. 2, pp. 27-32, 1998.

[8] D. O. Smallwood and D. Gregory, "Evaluation of a six-DOF electrodynamic shaker system," in *Proc. 79th Shock Vibration Symp.*, Orlando, FL, 2008.

[9] K. McIntosh and J. Davis, "Multi-axis testing of under wing and ground vehicle weapons systems," *Aerospace Testing International,* July 2002.

[10] U. Füllekrug and M. Sinapius, "Simulation of multi-axis vibration in the qualification process of space structures," in *Int. Symp. Env. Testing for Space Programmes*, Noordwijk, Netherlands, 1993.

[11] W. E. Whiteman and M. S. Berman, "Fatigue failure results for multi-axial versus uniaxial stress screen vibration testing," *Shock Vibration,* vol. 9, no. 6, pp. 319-328, 2002.

[12] E. Habtour, W. Connon, M. F. Pohland, S. C. Stanton, M. Paulus and A. Dasgupta, "Review of response and damage of linear and nonlinear

systems under multiaxial vibraiton," *Shock Vibration,* vol. 21, no. 4, 2014.

[13] D. Gregory, F. Bitsie and D. O. Smallwood, "Comparison of the response of a simple structure to single axis and multiple axis random vibration inputs," in *Proc. 79th Shock Vibration Symp.*, Orlando, FL, 2008.

[14] N. E. Loychik and J. Pan, "Achieving reliability goals for an EFV LRU through laboratory testing," in *Proc. Annu. Reliability Maintainability Symp.*, Lake Buena Vista, FL, 2011.

[15] H. Ling, F. Shichao and F. Yaoqi, "Effect of multi-axis versus single-axis vibration test on the dynamic responses of typical spacecraft structure," in *Proc. 25th Int. Conf. Noise Vibration Eng.*, Leuven, Belgium, 2012.

[16] R. M. French, R. Handy and H. L. Cooper, "A comparison of simultaneous and sequential single-axis durability testing," *Experimental Techniques,* vol. 30, no. 5, pp. 32-37, 2006.

[17] H. Himelblau, M. J. Hine, A. M. Frydman and P. A. Barrett, "Effects of triaxial and uniaxial random excitation on the vibration response and fatigue damage of typical spacecraft hardware," in *Proc. 66th Shock Vibration Symp.*, Biloxi, MS, 1995.

[18] M. Ernst, E. Habtour, A. Dasgupta, M. Pohland, M. Robeson and M. Paulus, "Comparison of electronic component durability under uniaxial and multiaxial random vibrations," *J. Electron. Packaging,* vol. 137, no. 1, p. 011009, 2015.

[19] C. Peterson, "Time-to-failure testing using single- and multi-axis vibraiton," *Sound Vibration,* vol. 47, no. 3, pp. 13-16, 2013.

[20] C. Harman and M. B. Pickel, "Multi-axis vibration reduces test time," *Evaluation Engineering,* June 2006.

[21] M. Aykan and M. Celik, "Vibration fatigue analysis and multi-axial effect in testing of aerospace structures," *Mech. Syst. Signal Process.,* vol. 23, no. 3, pp. 897-907, 2009.

[22] M. A. Underwood and M. Hale, "MIMO testing methodologies," in *Proc. 79th Shock Vibration Symp.*, Orlando, FL, 2008.

[23] Team Corporation, "Tensor 18kN multi-axis high frequency vibration test system," [Online]. Available: http://www.teamcorporation.com/images/brochures_A4/Tensor18kN_a4.pdf.

[24] L.D. Jacobs, M. Ross, G. Tipton, K. Cross, N. Hunter, J. Harvie, and G. Nelson, “6-DOF Shaker Test Input Derivation from Field Test.” To appear in the *Proceedings of the XXXV IMAC.*